

# Comparison of Numerical Modeling Techniques for Complex, Two-Dimensional, Transient Heat-Conduction Problems

B. G. THOMAS, I. V. SAMARASEKERA, and J. K. BRIMACOMBE

The accuracy, stability, and cost of the standard finite-element method, (Standard), Matrix method of Ohnaka, and alternating-direction, implicit finite-difference method (ADI) have been compared using analytical solutions for two problems approximating different stages in steel ingot processing. The Standard and Matrix methods both employ triangular elements and were compared using the Dupont, Lees, and Crank-Nicolson time-stepping techniques. Other variables include mesh and time-step refinement, type of boundary condition formulation, and the technique for simulating phase change. The best overall combination of methods investigated for modeling two-dimensional, transient, heat conduction problems involving irregular geometry was the Dupont-Matrix method with a lumped boundary condition formulation and temperature dependent properties evaluated at time level two, coupled with the Lemmon latent-heat evolution technique if phase change is involved. For problems with simple geometry, the ADI method was found to be more cost effective.

## I. INTRODUCTION

MANY numerical methods have been employed to solve for the temperature distribution in transient heat-conduction problems with or without change of phase. Traditionally, finite-difference techniques have been applied with considerable success; but as interest has grown in complex shapes and combined heat flow/stress problems, an example of which is the solidification of steel ingots with corrugations, attention has turned to finite-element methods developed originally for stress analysis of structures. As a result, the number of numerical methods and versions of each, available for use in tackling a given heat-flow problem, has increased rapidly; however, the comparative advantages of the different techniques with respect to accuracy, stability, and cost remain unclear. Thus, in the present paper, this question has been examined by comparing the temperature predictions of several different formulations of the standard finite-element method,<sup>1</sup> the matrix method of Ohnaka,<sup>2</sup> and the alternating-direction, implicit finite-difference method<sup>3</sup> against analytical solutions for two problems. Because this study is the first part of a larger project on heat flow and stress generation in steel ingots, the two problems have been chosen to approximate different stages in ingot processing: reheating in a soaking pit and solidification in the mold. These problems also test the ability of the numerical methods to handle temperature-dependent boundary conditions and the latent heat of solidification, respectively. Two-dimensional heat flow in the transverse mid-plane of the ingot has been considered.

## II. PROBLEMS STUDIED AND ANALYTICAL SOLUTIONS

### A. Reheating in a Soaking Pit

The first problem examined was the transient temperature distribution in the transverse section of a steel ingot

B. G. THOMAS, Graduate Student, I. V. SAMARASEKERA, Assistant Professor, and J. K. BRIMACOMBE, Stelco Professor of Process Metallurgy, are with the Department of Metallurgical Engineering, The University of British Columbia, Vancouver, B. C. V6T 1W5, Canada.

Manuscript submitted August 17, 1983.

(0.762 m × 1.524 m) "convectively" heated in a soaking pit, as shown in Figure 1. Heat was assumed to transfer uniformly to all four sides of the ingot, giving rise to a temperature distribution with two-fold symmetry; thus only one-quarter of the ingot section need be considered. The initial temperature of the ingot at charging,  $T_0$ , convective heat transfer coefficient,  $h$ , surrounding pit temperature,  $T_\infty$ , and thermophysical properties,  $k$ ,  $\rho$ , and  $C_p$ , were all assumed to be constant.

Heat conduction within the ingot then is described mathematically by the well-known partial differential equation\*

\*All symbols are defined in a Nomenclature section at the end of this paper.

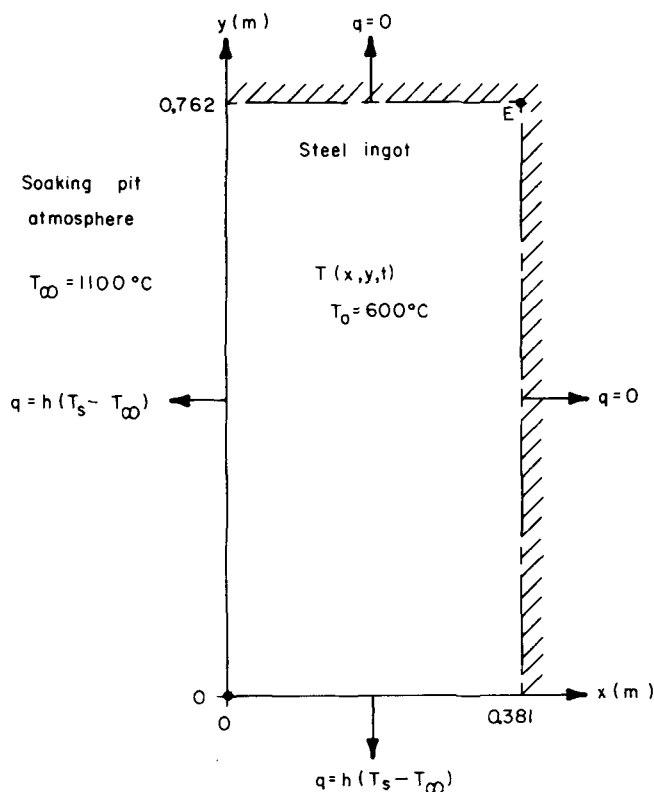


Fig. 1—Schematic diagram of first problem.

$$k\left(\frac{\partial^2 T}{\partial x^2} + \frac{\partial^2 T}{\partial y^2}\right) = \rho C_p \frac{\partial T}{\partial t} \quad [1]$$

applied over the two-dimensional, rectangular domain,

$$0 \leq x \leq 0.381 \quad [2]$$

$$0 \leq y \leq 0.762 \quad [3]$$

with the initial condition,

$$T = T_0 \quad [4]$$

and boundary conditions:

$$x = 0.381, \quad -\frac{k\partial T}{\partial x} = 0 \quad [5]$$

$$y = 0.762, \quad -\frac{k\partial T}{\partial y} = 0 \quad [6]$$

$$x = 0, \quad -\frac{k\partial T}{\partial x} = h(T_\infty - T) \quad [7]$$

$$y = 0, \quad -\frac{k\partial T}{\partial y} = h(T_\infty - T) \quad [8]$$

The analytical solution to this problem was obtained by the superposition of two one-dimensional series solutions from Luikov.<sup>4</sup> A sufficient number of terms were taken to ensure an estimated accuracy, with respect to the exact solution, of better than  $\pm 0.01$  pct for both short and long times. Values of the parameters used in the calculations are given in Table I.

### B. Solidification in the Mold

The second problem was concerned with the temperature distribution in a corner of the transverse section of the same steel ingot during the early stages of solidification in the mold as shown in Figure 2. Again symmetrical cooling was assumed so that only one-quarter of the ingot was considered. The temperature at the ingot/mold boundary,  $T_w$ , was taken to be fixed at  $1150^\circ\text{C}$ . The initial temperature of the molten steel was assigned a value of  $1535^\circ\text{C}$  which included a  $35^\circ\text{C}$  superheat over the unique solidification temperature,  $T_f$ , of  $1500^\circ\text{C}$ . Thermophysical properties were again taken to be constant.

The problem is expressed mathematically by the same governing equation, Eq. [1], domain, Eqs. [2] and [3], initial condition, Eq. [4], and first two boundary conditions, Eqs. [5] and [6], as the first problem, but includes the boundary conditions,

$$x = 0 \quad \text{and} \quad y = 0, \quad T = T_w \quad [9]$$

and additional conditions regarding the position of the

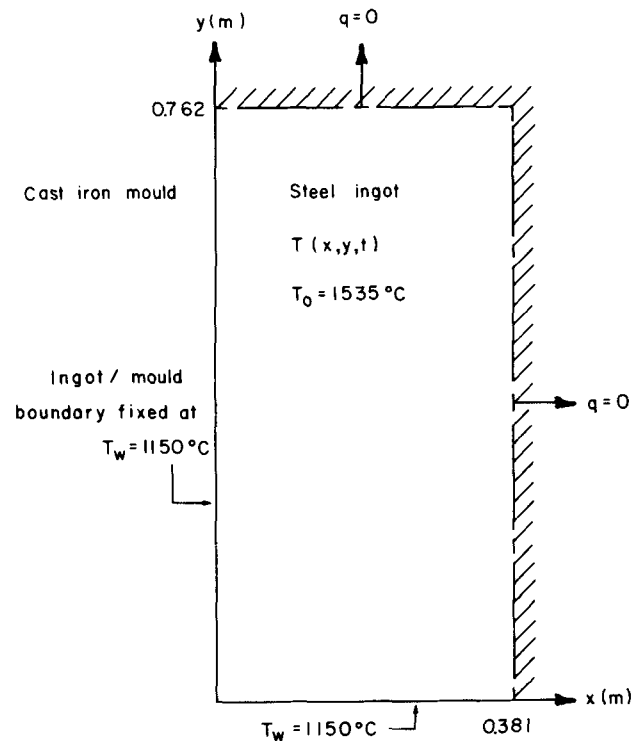


Fig. 2—Schematic diagram of second problem.

solidification front,  $S$ :

$$y = S(x, t), \quad T = T_f \quad [10]$$

$$k\left[\frac{\partial T}{\partial y}\Big|_{y=S^-} - \frac{\partial T}{\partial y}\Big|_{y=S^+}\right] \left[1 + \left(\frac{\partial S}{\partial x}\right)^2\right] = \rho H_s \frac{\partial S}{\partial t} \quad [11]$$

An approximate solution for this problem was obtained from the analytical solution of Rathjen and Jiji<sup>5</sup> for solidification in an unbounded corner. The problem is characterized, using their terms and parameters, by a dimensionless initial temperature,

$$T_i^* = \frac{T_0 - T_f}{T_f - T_w} = 0.1 \quad [12]$$

and a latent-to-sensible heat ratio,

$$\beta = \frac{H_s}{C_p(T_f - T_w)} = 1.0 \quad [13]$$

To retain an estimated accuracy in predicting temperatures of better than  $\pm 0.3$  pct, the applicability of this solution is restricted to times less than 6000 seconds. The progress of the solidification front with time, calculated from this solution for the conditions summarized in Table II, is illustrated in Figure 3.

### III. DESCRIPTION OF NUMERICAL METHODS TESTED

The numerical methods were formulated, for this study, to solve the general heat-conduction problem, Eq. [1], with one of the following three boundary conditions specified on each part of the boundary enclosing the region where temperatures are to be calculated:

(i) Neumann convective boundaries with specified heat

Table I. Conditions Assumed for First Problem of Ingot Reheating in a Soaking Pit

Ingot dimensions	0.762 m $\times$ 1.524 m
Initial steel temperature, $T_0$	$600^\circ\text{C}$ (uniform)
Thermal conductivity of steel, $k$	$30 \text{ W/m}^\circ\text{C}$
Density of steel, $\rho$	$7500 \text{ kg/m}^3$
Specific heat of steel, $C_p$	$800 \text{ J/kg}^\circ\text{C}$
Convective heat-transfer coefficient, $h$	$394 \text{ W/m}^2^\circ\text{C}$
Surrounding pit temperature, $T_\infty$	$1100^\circ\text{C}$

**Table II. Conditions Assumed for Second Problem of Ingot Solidification in a Mold**

Ingot dimensions	0.762 m × 1.524 m
Initial temperature of molten steel, $T_0$	1535 °C
Solidification temperature of steel, $T_f$	1500 °C
Thermal conductivity of steel,* $k$	30 W/m °C
Density of steel,* $\rho$	7200 kg/m <sup>3</sup>
Specific heat of steel,* $C_p$	750 J/kg °C
Latent heat of solidification, $H_s$	262.5 kJ/kg
Temperature of ingot/mold boundary, $T_w$	1150 °C

\*Thermophysical properties of liquid and solid steel are assumed to have the same values.

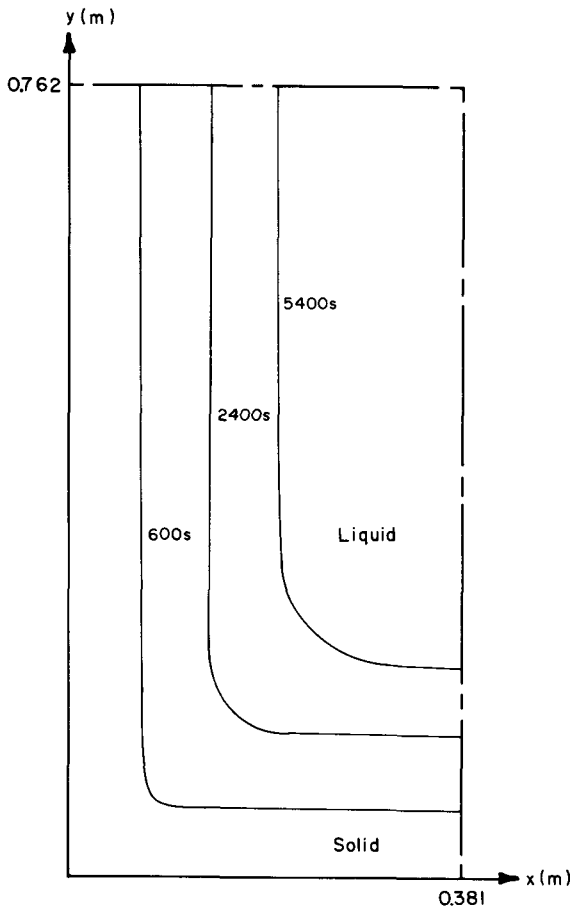


Fig. 3—Position of solidification front at different times from analytical solution to second problem.

transfer coefficient,  $h$ ,

$$-k \frac{\partial T}{\partial n} = h(T_\infty - T) \quad [14]$$

(ii) Neumann specified heat flux,  $q$ , boundaries,

$$-k \frac{\partial T}{\partial n} = q \quad [15]$$

(iii) Dirichlet fixed temperature boundaries,

$$T = T_w \quad [16]$$

where  $n$  is in a direction normal to the boundary. Thermophysical properties,  $k$ ,  $\rho$ , and  $C_p$ , are potentially functions of temperature and  $T_w$ ,  $T_\infty$  may be functions of time, while

$q$  and  $h$  may be both temperature and time dependent. In addition, the general problem is subject to the initial condition given by Eq. [4] where  $T_0$  may be a function of position.

Three different numerical methods were studied for solving the two, previously described, special cases of this problem. The alternating-direction implicit finite-difference (ADI) method of Peaceman and Rachford<sup>3</sup> was selected from the many finite-difference techniques available owing to its advantages (unconditional stability, second-order accuracy, and a cost-efficient solution algorithm involving tridiagonal matrices)<sup>6</sup> for two- and three-dimensional heat-conduction problems.<sup>7</sup> The ADI method then was used as a basis for comparison with the two finite-element methods studied in this investigation.

Finite-element methods have advantages over finite-difference schemes in problems involving complex geometry<sup>8</sup> and are more easily coupled with finite-element thermal stress models. The most widely used finite-element method, referred to here as the Standard Method, formulates element matrix equations by evaluating terms from general integral equations using element interpolation functions.<sup>1</sup>

The Matrix method of Ohnaka<sup>2</sup> is an alternate way to formulate the linear-temperature, three-node triangular element using a lumping procedure rather than the consistent distribution of the Standard method. It was chosen over other lumping schemes because the element equations are derived in a physically more logical manner by applying heat balances to the individual nodes.

#### A. Formulation of Finite-Element Methods

For the Standard and Matrix methods, the spatial continuum was discretized into three-node, linear-temperature, triangular elements as shown in Figure 4. Triangles were chosen over other shapes such as rectangles owing to their versatility in discretizing regions of complex shape. Higher order elements were not considered since for the ingot solidification problem it was felt that the discontinuous temperature field across the solid-liquid boundary would be better approximated by a large number of elements than by fewer elements each having more degrees of freedom.

By applying the finite-element method to the heat-conduction problem, *viz.*, Eqs. [1], [4], and [14] to [16], and summing the contributions from individual elements and boundaries,

$$[K] = \sum_{i=1}^E [K]_i^e + \sum_{i=1}^B [h]_i^b \quad [17]$$

$$[C] = \sum_{i=1}^E [C]_i^e \quad [18]$$

$$\{Q\} = \sum_{i=1}^B [\{Q\}_i^b - [h]_i^b \{T_\infty\}_i^b] \quad [19]$$

the following global matrix equation is obtained:

$$[K]\{T\} + [C]\{\dot{T}\} = \{Q\} \quad [20]$$

where  $\{\dot{T}\}$  contains the time derivatives of the unknown nodal temperatures,  $\{T\}$ . Equation [20] is solved at each time step using one of the techniques discussed in Section III-D.

The element conductivity matrix,  $[K]_i^e$ , is the same for both the Standard and Matrix methods, although the derivation for each is different. Applying the Standard method

Complete Coarse Mesh With Nodes

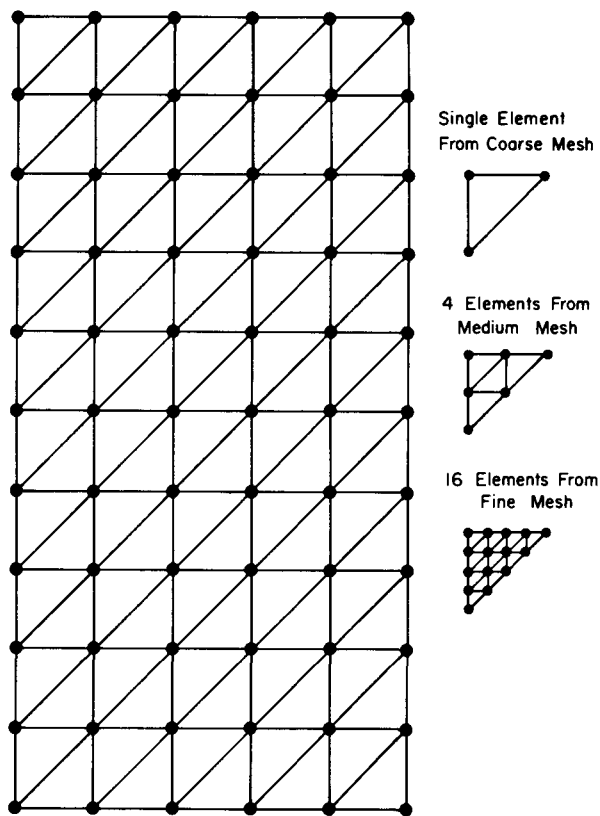


Fig. 4—Meshes used for numerical methods.

to the linear-temperature triangular element yields the following individual terms in the  $3 \times 3 [K]^e$  matrix:

$$K_{ij}^e = \frac{k}{2A}(b_i b_j + c_i c_j) \quad i, j = 1, 2, 3 \quad [21]$$

where:  $b_1 = y_2 - y_3$   
 $c_1 = x_3 - x_2$

and the other  $b_i$  and  $c_i$  values are obtained through cyclic permutation of the subscripts, 1, 2, 3 which represent the three nodes of the triangle having coordinates  $(x_1, y_1)$ ,  $(x_2, y_2)$ , and  $(x_3, y_3)$ , respectively. Although it is formulated by applying a finite-difference method to triangles, the element conductivity matrix obtained using the Matrix method is identical to that given by Eq. [21].

The only difference between the two methods is the formulation of the capacitance, or heat-storage matrix,  $[C]^e$ . Using the Standard method and assuming constant  $\rho C_p$  within the element results in a consistent  $3 \times 3 [C]^e$  matrix given by:

$$C_{ij}^e = \frac{\rho C_p A}{12} [1 + \delta_{ij}] \quad i, j = 1, 2, 3 \quad [22]$$

where  $\delta_{ij}$  is the Kronecker delta.

For the Matrix method,  $[C]^e$  is calculated by unequally distributing the capacitance to each node in proportion to its nodal area,  $A_i$ , which is defined by constructing perpendicular bisectors on each side of the triangle:

$$A_i = A/2 - \frac{1}{4}(a_i + b_i x_c + c_i y_c) \quad i = 1, 3 \quad [23]$$

where  $(x_c, y_c)$  are the coordinates of the centroid of the triangular element and  $a_i$  is defined in a similar manner to  $b_i$  and  $c_i$  with  $a_1 = x_2 y_3 - x_3 y_2$ . This results in a capacitance matrix in which terms are lumped along the main diagonal:

$$C_{ij}^e = \rho C_p A_i \delta_{ij} \quad i, j = 1, 2, 3 \quad [24]$$

### B. Formulation of Boundary Conditions

Four different methods for formulating the boundary conditions for the first problem were compared for each version of both the Standard and Matrix methods. A Neumann convective boundary is the natural choice and is accounted for in the finite-element methods by including the  $[h]^b$  matrix for each element side that forms part of the exterior boundary where Eq. [14] applies. Applying the Standard method assuming linear variation for  $T$  and  $h$  along the boundary results in the "linear  $h$  formulation":

$$h_{ij}^b = \frac{L(h_1 + h_2)}{12} + \frac{L h_i}{6} (\delta_{ij}) \quad i, j = 1, 2 \quad [25]$$

where  $L$  is the length of the boundary segment connecting nodes arbitrarily numbered 1 and 2.

Alternatively,  $[h]^b$  may be defined by "lumping"  $h$  at the two boundary nodes, giving rise to:

$$h_{ij}^b = \frac{h_i L}{2} (\delta_{ij}) \quad i, j = 1, 2 \quad [26]$$

This formulation, referred to as the "lumped  $h$  formulation", is more theoretically consistent with the Matrix method.

An alternative way to formulate the boundary conditions for the first problem is through the use of Neumann heat-flux boundaries (Eq. [15]). The finite-element methods account for these by incorporating a heat-flux vector,  $\{Q\}^b$ , for each appropriate boundary segment.

Applying the Standard method and assuming linear variation of both  $q$  and  $T$  along the boundary leads to the "linear  $q$  formulation":

$$Q_i^b = \frac{L}{6}(q_1 + q_2 + q_i) \quad i = 1, 2 \quad [27]$$

which is more compatible with the Standard method.

The final option, termed the "lumped  $q$  formulation", leads to:

$$Q_i^b = \frac{L q_i}{2} \quad i = 1, 2 \quad [28]$$

For the second problem, Dirichlet boundaries, Eq. [16], are required. The temperatures of nodes on these boundaries were effectively forced to assume desired values by employing the lumped  $h$  formulation with an arbitrarily large  $h$  (e.g.,  $10^9$ ).

### C. Methods of Latent-Heat Evolution

Accounting for latent-heat evolution is a difficult task for numerical methods, particularly when the phase-change temperature interval is small.<sup>9</sup> The problem has received a great deal of attention in recent literature. For problems dominated by latent-heat evolution, such as freezing soil, several researchers have developed methods of dynamically deforming the element grid system to maintain the finest mesh in the vicinity of the critical phase-change

region.<sup>10</sup> With these methods, the location of the solidification front is continually tracked. However, for the steel solidification problem involving important boundary heat flows, which is not dominated by latent heat effects, the extra complication and expense of these methods are not considered worthwhile.

For fixed-grid systems, where the solidification front is generally at an unknown location between nodes, two different classes of methods are available. The first treats latent heat as a temperature-dependent heat source term in the original heat-conduction equation, Eq. [1]. The temperature of each node<sup>11</sup> or element<sup>12</sup> undergoing phase change then is fixed at the solidification temperature until sufficient heat has been extracted to complete solidification and allow the solidification front to move on. These methods properly require iteration within a time step, however, and therefore were not considered further in this study.

The second group of methods treats the latent heat in terms of a temperature-dependent specific heat which, for finite-element methods, is included in the capacitance matrix  $[C]^e$  of the element.

Two types of the specific-heat method were evaluated in this investigation. The first is based on a temperature-dependent effective specific heat,  $\bar{C}_p$ , which is artificially raised above  $C_p$  over the phase-change temperature interval (PCTI) to account for latent heat:

$$\bar{C}_p = C_p + \frac{H_s}{T_{\text{liq}} - T_{\text{sol}}} \quad \text{for} \quad T_{\text{sol}} \leq T \leq T_{\text{liq}} \quad [29]$$

where  $T_{\text{liq}}$  and  $T_{\text{sol}}$  are the liquidus and solidus temperatures, respectively. For problems involving a unique solidification temperature such as the second problem outlined earlier, this method obviously requires the creation of an artificial PCTI about the true solidification temperature. To safeguard against nodes that "jump" over the PCTI in a single time step, and thus miss their latent-heat evolution, a post-iterative correction technique is used to readjust the temperatures of those nodes. This procedure, referred to as the "Specific-Heat method", is commonly used in finite-difference formulations<sup>7</sup> and therefore was the only latent-heat evolution technique employed with the ADI method. Because this method attributes a different  $\bar{C}_p$  to each individual node, rather than to the element, it was not considered applicable to the Standard finite-element method. However, it was used in conjunction with the Matrix method.

The second specific-heat method investigated is actually a sub-class of methods which calculates an effective specific heat for an entire element, through the use of an enthalpy function,  $H$ .

The first of these methods, evaluated in this investigation, was developed by Lemmon<sup>13</sup> in which

$$C_p = \left[ \frac{(\partial H/\partial x)^2 + (\partial H/\partial y)^2}{(\partial T/\partial x)^2 + (\partial T/\partial y)^2} \right]^{1/2} \quad [30]$$

where, for linear-temperature, triangular elements,

$$\partial H/\partial x = b_1 H_1 + b_2 H_2 + b_3 H_3 \quad [31]$$

$$\partial H/\partial y = c_1 H_1 + c_2 H_2 + c_3 H_3 \quad [32]$$

$$\partial T/\partial x = b_1 T_1 + b_2 T_2 + b_3 T_3 \quad [33]$$

$$\partial T/\partial y = c_1 T_1 + c_2 T_2 + c_3 T_3 \quad [34]$$

The second method, reported by Del-Giudice *et al.*,<sup>14</sup> gives the following relationship between  $C_p$  and  $H$ :

$$C_p = \left[ \frac{(\partial H/\partial x)(\partial T/\partial x) + (\partial H/\partial y)(\partial T/\partial y)}{(\partial T/\partial x)^2 + (\partial T/\partial y)^2} \right] \quad [35]$$

In both methods, if the denominator equals zero, the temperature is constant throughout the element and the appropriate  $C_p$  can easily be determined. The use of a PCTI is optional for these methods. A third method developed by Comini *et al.*<sup>15</sup> uses

$$C_p = \frac{1}{2} \left[ \frac{\partial H/\partial x}{\partial T/\partial x} + \frac{\partial H/\partial y}{\partial T/\partial y} \right] \quad [36]$$

but was not considered in this work because Del-Giudice *et al.*<sup>14</sup> found it to be inferior to that given by Eq. [35].

#### D. Time-Stepping Techniques

The system of discrete first-order, nonlinear, differential equations obtained from the finite-element, semi-discretization of space, given by the matrix equation, Eq. [20], was solved incrementally using a finite-difference approximation in the time domain. Although several investigators have used finite elements in time,<sup>16,17</sup> finite-difference recurrence relationships, a great many of which are in the literature, are usually employed. Of these, three different time-stepping algorithms were investigated. They are distinguished by the way in which  $\{T\}$  and  $\{\dot{T}\}$  are evaluated in terms of temperatures at known and unknown time levels.

The first method investigated was the Dupont three-level technique<sup>18</sup> (Dupont):

$$[K] \left\{ \frac{3T_3 + T_1}{4} \right\} + [C] \left\{ \frac{T_3 - T_1}{2\Delta t} \right\} = \{Q\} \quad [37]$$

Solving for the unknown temperatures at the third time level yields

$$\{T_3\} = \left[ \frac{[C]}{\Delta t} + \frac{3[K]}{4} \right]^{-1} \left[ \frac{[C]}{\Delta t} \{T_2\} - \frac{[K]}{4} \{T_1\} + \{Q\} \right] \quad [38]$$

This method is one of a class of second-order accurate, three-level techniques developed by Dupont *et al.*<sup>18</sup> and is referred to by Hogge<sup>19</sup> as the "Dupont II scheme with  $\alpha = 1/4$ ". It was chosen because Hogge reported its overall performance in accuracy and stability to be superior to other time-stepping methods in solving the one dimensional, homogeneous equation:

$$kT + \dot{T} = 0 \quad [39]$$

where  $k$  has a slight linear temperature dependence. The Dupont method has unconditional  $A_0$  stability;<sup>19,20</sup> but in a theoretical study on the stability of various time-stepping techniques in solving Eq. [39] with constant  $k$ , Wood<sup>20</sup> has demonstrated that any three-level method which is  $A_0$  stable cannot guarantee all real eigenvalues, so is termed "relatively unstable". This means that the Dupont method could be prone to oscillation under certain circumstances.

The second method tested was the Lees three-level technique<sup>21</sup> (Lees)

$$[K] \left\{ \frac{T_1 + T_2 + T_3}{3} \right\} + [C] \left\{ \frac{T_3 - T_1}{2\Delta t} \right\} = \{Q\} \quad [40]$$

Again solving for the unknown temperatures at the third time level gives

$$\{T_3\} = \left[ \frac{[K]}{3} + \frac{[C]}{2\Delta t} \right]^{-1} \cdot \left[ -\frac{[K]}{3}\{T_2\} - \frac{[K]}{3}\{T_1\} + \frac{[C]}{2\Delta t}\{T_1\} + \{Q\} \right] \quad [41]$$

This method was chosen because it has been used successfully by several investigators<sup>14,15,22,23</sup> in modeling nonlinear, metallurgical heat-transfer problems. Like the Dupont method, it has unconditional  $A_0$  stability but is relatively unstable for both very small and very large time steps.<sup>20</sup>

The final method tested was the Crank-Nicolson two-level technique<sup>24</sup> (C-N):

$$[K] \left\{ \frac{T_2 + T_1}{2} \right\} + [C] \left\{ \frac{T_2 - T_1}{\Delta t} \right\} = \{Q\} \quad [42]$$

Solving for the unknown temperatures at the second time level yields:

$$\{T_2\} = \left[ \frac{[K]}{2} + \frac{[C]}{\Delta t} \right]^{-1} \left[ -\frac{[K]}{2}\{T_1\} + \frac{[C]}{\Delta t}\{T_1\} + \{Q\} \right] \quad [43]$$

This well known, two-level technique was chosen for comparison with the three-level schemes, and additionally was used to generate second-level temperatures to start the three-level methods. C-N is the only second-order accurate, two-level scheme and has zero stability,  $A_0$  stability, and relative stability.<sup>20</sup> However, its stability is only marginal so that this method also is prone to oscillation if large time steps are used.<sup>20,25</sup>

For highly nonlinear problems, several researchers have employed secant or tangent methods which involve iteration within each time step.<sup>26-29</sup> These methods have been compared by Hogge<sup>30</sup> and are expensive, particularly in the case of the tangent method in which new  $[K]$  and  $[C]$  matrices are constructed every iteration. Since a steel ingot solidification problem is only mildly nonlinear, these methods were not considered to be justified economically. However, they may have useful application for solidification problems dominated by highly nonlinear latent-heat effects.

No iteration was done within time steps in this investigation. Thus, the calculation of temperature dependent, or nonlinear terms in  $[K]$ ,  $[C]$ , and  $\{Q\}$ , requires the use of temperatures,  $\{T_n\}$ , evaluated at preceding time levels. In the first problem,  $\{Q\}$  is nonlinear for the specified  $q$  formulation owing to its dependence on the surface temperature,  $T_s$ . In the second problem,  $[C]$  is nonlinear due to the temperature dependence of the specific heat,  $C_p$ .

For the ADI and C-N methods, these calculations must be performed using temperatures from the first-time level,  $\{T_*(t_1)\}$ . However, the Dupont and Lees methods may employ any linear combination of temperatures from the first and second time levels. In this study, the following five cases were investigated:

$$T_*(t_1) = T(t_1) \quad [44]$$

$$T_*(t_{1.5}) = 0.5T(t_1) + 0.5T(t_2) \quad [45]$$

$$T_*(t_2) = T(t_2) \quad [46]$$

$$T_*(t_{2.5}) = 1.5T(t_2) - 0.5T(t_1) \quad [47]$$

$$T_*(t_3) = 2.0T(t_2) - T(t_1) \quad [48]$$

From a theoretical standpoint,  $T_*$  should be evaluated at  $t_2$  for the Lees method<sup>19,22</sup> and at  $t_{2.5}$  for the Dupont method.<sup>19</sup>

Using these techniques, the matrix equations resulting from Eqs. [38], [41], and [43] can be written in the form:

$$[M]\{T\} = \{F\} \quad [49]$$

Since  $[M]$  is a positive definite, symmetric, banded matrix, the equation can be solved efficiently at each time step using the Cholesky method.<sup>31</sup>

#### IV. COMPARISON METHODOLOGY

To compare the finite-element and the ADI methods on an equal basis, one-fourth of the ingot section (0.381 m  $\times$  0.762 m) was discretized into a rectangular grid of nodes. For the Standard and Matrix methods, the nodes were then connected to form a mesh of three-node, right-angled, triangular elements. Three meshes, shown in Figure 4, were employed: a coarse, 6  $\times$  11 mesh with 66 nodes and 100 elements, a medium 11  $\times$  21 mesh with 231 nodes and 400 elements, and a fine 21  $\times$  42 mesh with 861 nodes and 1600 elements. It should be noted that each refinement of the mesh completely contains all coarser meshes. Care was taken in numbering the nodes to ensure that the band width of  $[M]$  was minimized. The numerical methods were coded as Fortran IV programs that were made to be as similar and efficient as possible. The programs were run on an Amdahl 470 V/8, 12-megabyte computer at the University of British Columbia.

The analytical solutions were used to calculate nearly exact temperatures  $\{T_a\}$  for each node in the mesh at 600-second time intervals for both test problems investigated. Percent differences between the "exact" temperatures and numerically generated values,  $\{T_n\}$ , were calculated for each node at these time intervals.

Two criteria were established to compare the relative accuracy of the various methods at each time step:

(i) average absolute value of percent error:

$$1/N \sum_{i=1}^N \left| \frac{T_n - T_a}{T_a} \right| \times 100 \text{ pct} \quad [50]$$

(ii) maximum percent error from the set of  $N$  nodal errors in Eq. [50].

For problems involving solidification such as the second problem, many previous investigators have based the comparison of numerical and analytical solutions on the position of the solidification front. However, errors in actual temperature predictions are more sensitive, and therefore have been used as the criterion for comparison. Their accuracy is also of practical importance because the thermal stress calculations require these temperatures.

Stability was estimated by visually examining the behavior of the maximum absolute percent error with increasing time, and assigning an "instability index" of 0 to 3 in order of increasing instability as follows:

0 = completely stable, with maximum error decreasing monotonically with time.

1 = stable with a fluctuating maximum error that eventually decreases.

2 = unstable, with a fluctuating maximum error that gradually increases out of control.

3 = extremely unstable, with average error exceeding 100 pct after only a few time steps.

Costs for each method were estimated by considering both CPU time and core storage.

## V. RESULTS AND DISCUSSION

Each numerical method generated many nodal temperatures at every time step of the simulation from which average and maximum percent errors were calculated. For comparative purposes, it was desirable to characterize the overall accuracy of each method using errors calculated at only a single time step. Extensive examination of the location of the node with the maximum error has consistently revealed that errors in temperature predictions are proportional to the temperature gradient, regardless of the method, mesh, and time step used. Because temperatures are changing the most rapidly early in the simulation, average and maximum errors at 600 seconds have been singled out to characterize accuracy for both problems as shown in Tables III and IV and Figure 5.

### A. Size of Mesh and Time Step

#### 1. Effect on accuracy

The influence of mesh refinement and time-step size on accuracy can be seen by examining Figure 5. This figure shows the typical effects of these variables on average error using equivalent formulations of the Standard and Matrix methods as examples. Unless stability problems are encountered, accuracy generally improves with refinement of both mesh and time step. However, until the time-step size is reduced below a critical value, mesh refinement does not lead to improvement, as accuracy is similar among all three meshes for large time steps. Once the time step is smaller than the critical value, finer meshes greatly improve accuracy. This critical time-step size is smaller for finer meshes. Continued refinement of the time-step size (*i.e.*, increase in the number of time steps taken to reach 600 seconds) results in little further improvement and eventually the accuracy worsens. Thus, every given mesh has an inherent limit in achievable accuracy and an optimum range of time-step size associated with it.

Time-step size optima have been reported elsewhere in previous studies comparing numerical methods.<sup>16,32</sup> Gray and Schnurr<sup>32</sup> found such optima only when using the finite-element method and postulated that any increase in error with increasing degrees of freedom was due to simple computational round-off error. However, Keramidas<sup>16</sup> attributed the optima to the space and time approximations inherent in the numerical methods. He found sharp, distinct optima to occur at a constant value of dimensionless  $\Delta t/\Delta x$  of 0.5 in a study of a simplified, one-dimensional, heat-conduction problem involving a first-order partial differential equation formulated in terms of heat displacement,  $U$ , where  $T = \partial U/\partial x$ . It was stated that for a more conventional formulation, the parameter for error and stability control should instead be  $\Delta t/\Delta x^2$ .

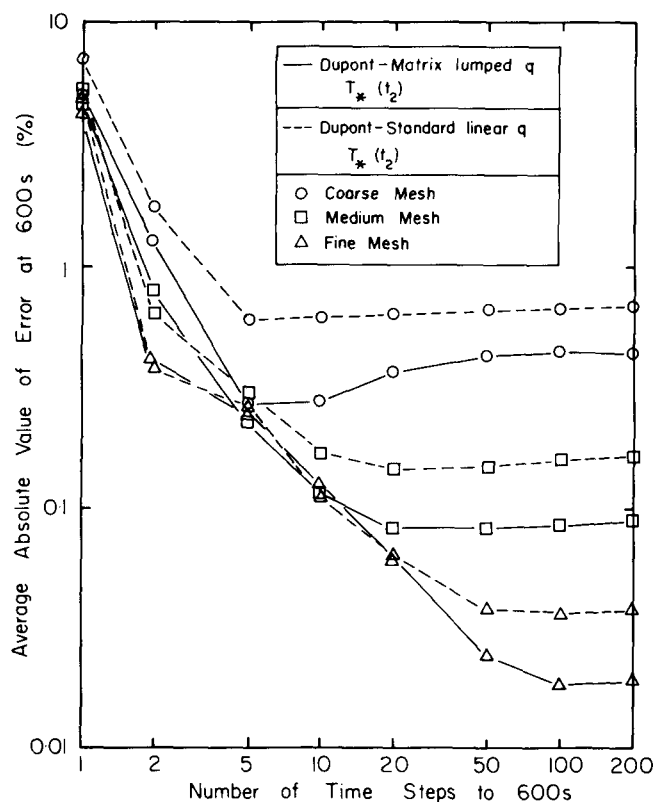


Fig. 5—Effect of size of mesh and time step on accuracy for first problem.

In the present study, time-step size optima were found for every method tested, including the ADI. Unfortunately, the optimum values varied with the method, were problem dependent, and often were not distinct. Thus, a precise relationship between the mesh size and optimum time-step size was difficult to establish in general. However, the optimum does occur at smaller time steps with finer meshes; and the dimensionless parameter,  $(k/\rho C_p) \Delta t/(\Delta x)^2$  appears to remain constant with a value of roughly 0.1 at the optimum of each of the three meshes examined. It is important to emphasize that increasing refinement of the time-step size for a given mesh does not continuously improve accuracy, but it does steadily raise computing costs.

#### 2. Effect on stability

For the linear problem, *i.e.*, the first problem formulated with  $h$  boundaries, all the numerical methods remained stable with time steps at least up to 4800 seconds although the accuracy became unacceptably poor with higher values of  $\Delta t$ . In the case of the nonlinear problems which included all other formulations of the first problem and all formulations of the second problem ( $\{Q\}$  and  $[C]$  are temperature dependent) every method examined eventually became unstable if the time step was made sufficiently large. However, instability was much less severe with the second problem since it was formulated with fixed-temperature boundaries. Instability was found for time steps in excess of 300 seconds for both the Lees and C-N methods; for ADI, instability occurred at time steps of 600 seconds or more. The Dupont method is the most stable, as its stability was retained for time steps up to 1200 seconds. These values pose upper limits to stability since they were determined for the optimum formulation of each method. They are independent

Table III. Accuracy and Stability of Numerical Methods for First Problem

Boundary Condition Formulation	$T_*$	Dupont Matrix	Dupont Standard	Lees Matrix	Lees Standard	C-N Matrix	C-N Standard	ADI
Lumped $h$	—	0.43	0.53	0.52	0.58	0.37	0.47	0.08
		1.6	1.8	2.1	1.9	1.6	1.4	0.3
		0	0	0	0	0	0	0
Linear $h$	—	0.43	0.54	0.52	0.56	0.38	0.47	
		1.7	1.8	2.1	1.9	1.6	1.4	
		0	0	0	0	0	0	
Lumped $q$	$t_1$	0.87	0.62	0.69	1.51	0.31	0.44	0.31
		4.7	4.2	11.3	67.4	1.2	28.4	1.2
		0	1	1	3	0	3	0
	$t_{1.5}$	0.54	0.52	0.27	0.31			
		2.8	5.6	1.1	14.6			
		0	0	0	2			
	$t_2$	0.23	0.29	1.13	2.77	← average error (pct)		
		1.1	1.5	38.9	189.4	← maximum error (pct)		
		0	1	3	3	← instability index		
	$t_{2.5}$	0.15		5.65				
		0.7		243.0				
		0		3				
	$t_3$	0.43						
		1.6						
		0						
Linear $q$	$t_1$	0.85	0.62	0.68	1.42	0.31	0.34	
		4.6	4.1	8.1	44.1	1.9	11.4	
		0	0	1	3	0	1	
	$t_{1.5}$	0.54	0.51	0.27	0.25			
		2.7	4.3	1.3	5.4			
		0	0	0	1			
	$t_2$	0.23	0.29	1.07	2.29			
		1.7	2.9	26.9	91.1			
		0	0	3	3			
	$t_{2.5}$		0.24		13.17			
			1.3		630.3			
			0		3			
	$t_3$		0.55					
			12.1					
			0					

Evaluated for medium mesh with time step—120 seconds  
Average and maximum errors recorded at 600 seconds

of the mesh used and are slightly lower for the Standard method, as compared with the Matrix method, which is more stable.

### 3. Grading of mesh and time step

The results in the preceding sections have been obtained with constant time steps and a uniform mesh. Accuracy may be improved, however, if the mesh is refined in regions which experience rapid temperature changes or if the time step is reduced during periods when the temperature changes quickly. An example of improved accuracy achieved by using smaller time steps early in the simulation of the first problem is shown in Figure 6. Other calculations revealed that grading the time steps in this way consistently resulted in improved accuracy over constant time steps for an equal number of iterations, and had no adverse effect on stability provided that time-step limits were not exceeded. Thus significant cost savings are possible in solving real prob-

lems.<sup>15</sup> However, grading the mesh by using finer elements near the surface was found to be much less advantageous. While accuracy close to the surface improved, increased errors resulted in the interior with no net significant improvement in accuracy for the two graded mesh configurations tested. In addition, the use of a graded mesh increased the tendency toward instability. Although the benefits of mesh refinement should not be disregarded, these results indicate that considerable care must be taken in selecting a graded mesh. In particular, elements with excessive aspect ratios must be avoided.

## B. Comparison of Numerical Methods

### 1. Accuracy and stability

The accuracy and stability of the numerical methods tested are presented in Tables III and IV. For comparative purposes, a constant time step of 120 seconds was selected



**Table IV. Accuracy and Stability of Numerical Methods for Second Problem**

Solidification Method	$T_s$	Dupont Matrix	Dupont Standard	Lees Matrix	Lees Standard	C-N Matrix	C-N Standard	ADI	
Specific heat	$t_1$					0.16		0.36	
						1.2		2.8	
					3		1		1
	$t_{1.5}$	3		3					
	$t_2$	0.15							
		1.1							
		1		3					
	$t_{2.5}$	3							
Lemmon	$t_1$			0.26	0.63	0.13	0.39		
				5.1	5.7	3.1	2.9		
				1	1	1	1		
	$t_{1.5}$	0.28	0.38	0.11	0.24				
		3.8	2.6	2.8	1.9				
		1	1	1	1				
	$t_2$	0.12	0.43	0.17	0.45				
		1.5	2.9	3.7	5.5	← average error (pct)			
		1	1	2	2	← maximum error (pct)	← instability index		
	$t_{2.5}$	0.21	0.43						
		3.0	3.8						
		1	1						
Del-Giudice	$t_1$			0.26	0.64	0.24	0.41		
				5.0	6.0	3.6	4.0		
				1	1	1	1		
	$t_{1.5}$	0.28	0.40	0.12	0.25				
		3.8	3.8	2.8	1.9				
		1	1	1	1				
	$t_2$	0.14	0.46	0.19	0.45				
		2.9	3.8	4.6	5.6				
		1	1	2	2				
	$t_{2.5}$	0.22	0.45						
		3.8	4.5						
		1	1						

Phase change temperature interval = 20 °C for specific heat technique  
 = 2 °C for Lemmon and Del-Giudice  
 Evaluated for medium mesh with time step = 30 seconds  
 Average and maximum errors recorded at 600 seconds

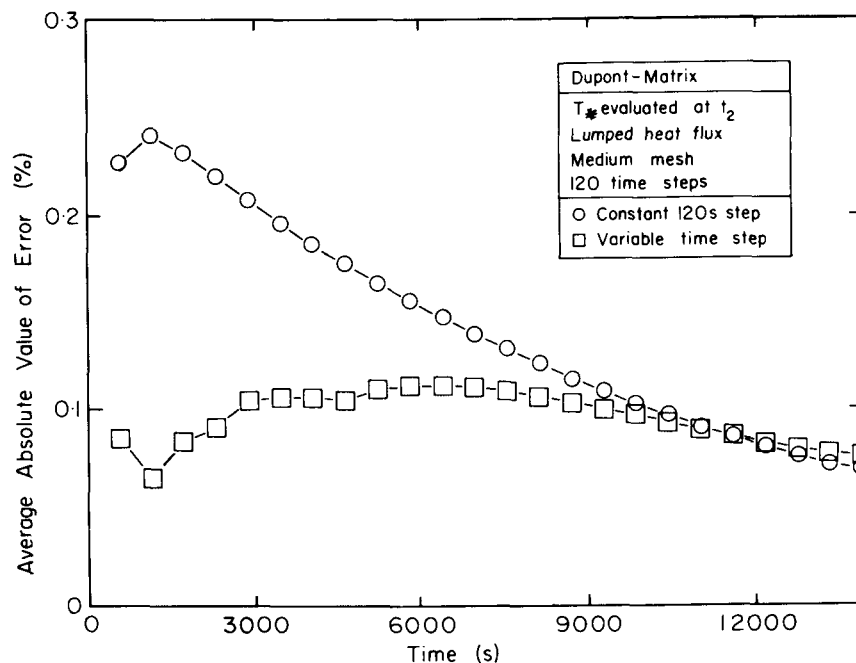


Fig. 6—Accuracy improvement using variable time steps.

for the first problem and 30 seconds for the second problem in conjunction with a regular, medium mesh. These conditions were chosen because they generally produced a reasonable accuracy of less than 1 pct average error at 600 seconds for both problems. In addition, the results in Tables III and IV are representative of the comparisons made over the entire spectrum of mesh and time-step sizes examined.

Although each of the seven methods compared can solve either problem effectively if formulated optimally, some have distinct advantages over others. Tables III and IV and Figure 5 show that the Matrix method has better accuracy and stability than the Standard finite-element method, although their performance is generally quite similar. Since it represents an upper bound to the eigenvalues, the Standard method, with its consistent  $[C]$  matrix, has a greater tendency toward oscillation for short time steps when steep temperature gradients are present.<sup>33,34</sup> This is seen in Table III pertaining to the first problem where higher values of the instability index are listed for the Standard method, particularly for the Lees and C-N time-stepping techniques. In the second problem, Table IV, stability of the Standard and Matrix methods is similar, but the accuracy of the Matrix method is clearly superior.

Very little difference is seen between the lumped and linear boundary condition formulations in Table III. Average errors are the same, but maximum errors are slightly higher for the linear formulation. Since there is no difference in stability between them for the Matrix method, it would seem better to formulate the Matrix method using the lumped formulation. However, the Standard method exhibits slightly increased instability with the lumped formulation and is better with the linear formulation. These findings are consistent with the theoretical bases of these methods.

The single, most important variable affecting stability and accuracy for both problems is the choice of time level at which  $T_*$  is evaluated for the three-level methods. Tables III and IV indicate that the optimum choice, although different for each time-stepping technique, is the same for each problem. This is especially significant because the nonlinearity occurs in different places for each problem; temperature dependencies occur only in  $\{Q\}$  for the first problem and in  $[C]$  for the second.

The Lees method has acceptable stability only at  $T_*(t_{1.5})$ . In fact, with the mesh and time-step size used in Table III, it became unstable (instability index  $\geq 2$ ) for every choice other than  $T_*(t_{1.5})$ . In addition, optimum accuracy occurs at  $T_*(t_{1.5})$ . This finding is contrary to the theoretical predictions of Bonacina *et al.*<sup>22</sup> that the best result should be obtained at  $T_*(t_2)$ .

The Dupont method, on the other hand, has excellent stability for all ways of calculating  $T_*$ . Its accuracy is at an optimum for  $T_*(t_{2.5})$  in the first problem and is best at  $T_*(t_2)$  for the second. However, when the time level exceeded  $t_2$  for the first problem, the method became unstable beyond time steps of 600 seconds. Recalling that the optimum Dupont method, evaluated using  $T_*(t_2)$ , did not become unstable until greater than 1200 seconds,  $T_*(t_2)$  is the safer overall choice. This is again contrary to the theoretical analysis that  $T_*$  should be evaluated at  $t_{2.5}$ .<sup>19</sup>

The results in Tables III and IV combined with the previous discussion of upper limits to time steps, indicate that the Dupont method has much better stability than that of

Lees. This agrees with the findings of Hogge<sup>19</sup> and Wood<sup>20</sup> that the Lees method is more prone to oscillation and instability. In addition, Tables III and IV show that the Dupont method is slightly more accurate than the Lees.

The C-N two-level, time-stepping method has been used as a basis for comparison by several investigators.<sup>35,36,37</sup> In this investigation, its performance was surprisingly good, particularly with the Matrix method. Tables III and IV show its accuracy and stability to be close to that of the best formulations of the Dupont and Lees methods.

Three different methods for handling latent-heat evolution are compared in Table IV. To enable implementation of the Specific-Heat method in the second problem, involving a unique solidification temperature, an artificial phase change temperature interval (PCTI) was created. Although it should theoretically equal zero for the other methods, Figure 7 shows the effect on accuracy of varying PCTI up to 50 °C for all three methods. The Dupont-Matrix method with  $T_*(t_2)$  was chosen for illustrative purposes. As one would expect, error generally rises as PCTI is increased. The Del-Giudice method yields the lowest error at a PCTI of about 5 °C while the Specific-Heat method has a minimum at 20 °C. When PCTI is increased above 30 °C, all three methods predict roughly the same temperatures.

Accuracy is not very dependent on changes in PCTI for any of the methods. However, without the post-iterative correction, the Specific-Heat method is extremely sensitive to the PCTI, and accuracy deteriorates rapidly when it is reduced to below 30 °C. Table IV shows that the Specific-Heat method is prone to serious instability problems for all

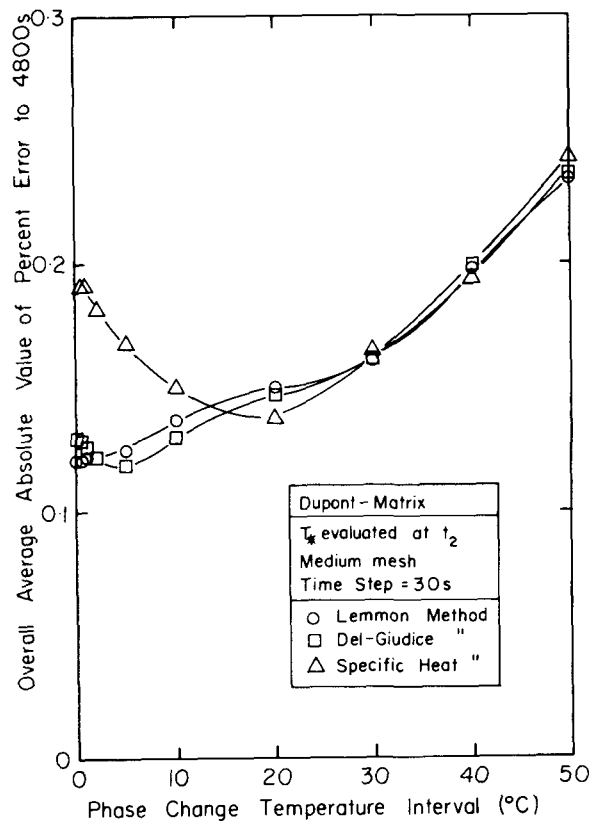


Fig. 7—Effect of varying phase change temperature interval (PCTI) on accuracy for second problem.

but the best time-stepping methods: Dupont with  $T_*(t_2)$ , C-N, and ADI. In addition, its accuracy even at the optimum PCTI of 20 °C is slightly worse than that of the other methods at their best. Thus, the enthalpy methods seem better suited for finite-element predictions of latent-heat evolution.

Table IV and Figure 7 also show that the Lemmon and Del-Giudice methods are very similar with respect to both stability and average error. However, the Lemmon method has slightly lower maximum errors and is the only method whose error is lowest at the PCTI of zero. In addition, its accuracy increases more rapidly than that of Del-Giudice with time-step refinement. The Lemmon method, therefore, is recommended for an ingot solidification problem.

Since the second problem studied with zero PCTI was actually a more difficult challenge for the numerical methods, temperature predictions for a steel ingot, where the PCTI is about 25 °C, are expected to be quite accurate.

## 2. Costs

The cost per time step was almost identical for every finite-element method tested, regardless of its formulation. It was independent of the number of time steps but rose markedly with mesh refinement. Table V compares the cost per time step of the finite-element methods with that of ADI for each of the three meshes used. The ADI method is seen to have a large cost advantage, both in CPU time and VM storage, which agrees with the findings of several previous investigators.<sup>2,38,39</sup> The cost of the ADI method is only one-third that of the other methods and, in addition, increases less rapidly with mesh refinement.

Moreover, Table III indicates that ADI has comparable accuracy to the finite-element methods when a  $q$  formulation is used and is five times more accurate for the  $h$  formulation. Although not quite as accurate for the second problem, it might be improved if enthalpy methods were implemented.<sup>40</sup> Finally, its stability is comparable to the best of the finite-element methods. Thus, the ADI finite-difference method is the most cost-effective method evaluated in this investigation.

## VI. CONCLUSIONS

From this comparative study of numerical methods for complex, transient, heat-conduction problems, the following conclusions can be drawn:

1. For heat-flow problems involving irregular geometry (such as steel ingots with corrugations), the Dupont-Matrix method with a lumped boundary-condition

formulation and  $T_*(t_2)$  coupled with the Lemmon latent-heat technique, if change of phase is involved, has the best stability and accuracy of all combinations of methods tested.

2. For problems with a simple geometry, the ADI finite-difference method coupled with the Specific-Heat, latent-heat technique is more cost-effective with stability and accuracy similar to the finite-element methods.
3. Using a finer mesh gives little or no improvement unless employed in conjunction with fine time steps. Every given mesh has an inherent limit in achievable accuracy, and continuous refinement of the time-step size does not continuously increase the accuracy.
4. The use of graded time steps with the finite-element method is very beneficial but the advantages from grading the mesh are more difficult to achieve.
5. The Dupont three-level time-stepping scheme is clearly superior to that of Lees in both accuracy and stability.
6. Temperature-dependent terms should be evaluated using  $T_*(t_{1,5})$  for the Lees time-stepping method and  $T_*(t_2)$  for the Dupont method.
7. The Matrix method consistently has slightly better accuracy and stability than the Standard finite-element method.
8. A linearly distributed boundary condition formulation should be used in conjunction with the Standard method while a lumped formulation is slightly better for the Matrix method.
9. The Lemmon method is the best latent-heat evolution technique but is only slightly better than that of Del-Giudice. The effect of varying phase change temperature interval is small.
10. The C-N two-level time stepping method is comparable in both accuracy and stability with the three-level schemes. Thus, further study is recommended into the use of two-level schemes, particularly for solidification problems, where iteration within a time step and cost-saving, explicit schemes might prove to be beneficial.

## NOMENCLATURE

- $A$  area of element ( $m^2$ )  
 $A_i$  nodal area ( $m^2$ )  
 $a_i$  parameter in natural coordinate functions  
 $B$  number of external boundaries  
 $b$  pertaining to external element boundary  
 $b_i$  parameter in natural coordinate functions  
 $[C]$  global capacitance matrix

Table V. Estimated Computer Costs per Time Step

Mesh	Number of Nodes	Number of Elements	Method	CPU Time (Seconds)	Core Storage (Megabytes)	Cost* (Cents)
Coarse	66	100	Standard and Matrix	0.032	0.071	0.29
			ADI	0.012	0.024	0.11
Medium	231	400	Standard and Matrix	0.141	0.129	1.31
			ADI	0.042	0.038	0.38
Fine	861	1600	Standard and Matrix	0.743	0.416	7.60
			ADI	0.154	0.088	1.41

\*Based on = 8.88¢/CPU s and 3.25¢/megabyte-s  
or cost = (CPU time) [8.88 + 3.25 (core storage)]

$[C]^e$  element capacitance matrix  
 $C_p$  specific heat of steel (J/kg °C)  
 $\bar{C}_p$  effective specific heat  
 $c_i$  parameter in natural coordinate functions  
 $E$  number of elements  
 $e$  pertaining to element  
 $\{F\}$  thermal "force" vector in Eq. [49]  
 $H$  enthalpy (J/kg)  
 $H_s$  latent heat of solidification (J/kg)  
 $h$  heat transfer coefficient (W/m<sup>2</sup> °C)  
 $[h]^b$  heat transfer coefficient matrix  
 $[K]$  global conductivity matrix  
 $[K]^e$  element conductivity matrix  
 $k$  steel thermal conductivity (W/m °C)  
 $L$  length of element boundary (m)  
 $[M]$  global coefficient matrix in Eq. [49]  
 $N$  number of nodes in mesh  
 $\{Q\}$  global thermal force vector  
 $\{Q\}^b$  boundary heat flux vector  
 $q$  heat flux (W/m<sup>2</sup>)  
 $S$  position of phase change boundary (function describing location of solidification front)  
 $T$  temperature (°C)  
 $\dot{T}$  time derivative of temperature  $\partial T/\partial t$   
 $T_0$  initial temperature  
 $T_\infty$  surrounding temperature  
 $T_w$  fixed wall temperature  
 $T_s$  surface temperature  
 $T_f$  fusion temperature  
 $T_i^*$  dimensionless initial temperature  
 $T_a$  analytical calculated temperature  
 $T_n$  numerically calculated temperature  
 $T_*$  temperature at which temperature-dependent terms in  $[K]$ ,  $[C]$ , and  $\{Q\}$  are evaluated  
 $t$  time (s)  
 $\Delta t$  time step  
 $x, y$  coordinate directions (m)  
 $x_c, y_c$  centroid of triangle  
 $U$  temperature displacement  
 $\beta$  latent to sensible heat ratio  
 $\delta_{ij}$  Kronecker delta  $\begin{cases} 1 & \text{if } i = j \\ 0 & \text{if } i \neq j \end{cases}$   
 $\rho$  steel density (kg/m<sup>3</sup>)  
 $[ ]$  square matrix  
 $\{ \}$  column vector  
 $[ ]^T$  transpose of matrix  
 $[ ]^{-1}$  inverse of matrix

## ACKNOWLEDGMENTS

The authors are most grateful to Stelco Inc. for the support of research expenses and to Noranda and the Natural Sciences and Engineering Research Council of Canada for fellowships granted to BGT.

## REFERENCES

- O. Zienkiewicz: *The Finite Element Method*, 3rd edn., McGraw-Hill, London, 1977, pp. 1-11, 164-68, 423-30, 527-39.
- I. Ohnaka and T. Fukusako: *Trans. Iron Steel Inst. Japan*, 1977, vol. 17, pp. 410-18.
- D. Peaceman and H. Rachford: *J. Soc. Indust. Appl. Math.*, 1955, vol. 3, pp. 28-41.
- A. Luikov: *Analytical Heat Diffusion Theory*, Academic Press, New York, NY, 1968, pp. 214-40.
- K. Rathjen and L. Jiji: *Journal of Heat Transfer*, Trans. ASME, 1971, vol. 93, pp. 101-09.
- B. Carnahan, H. Luther, and J. Wilkes: *Applied Numerical Methods*, John Wiley and Sons, Inc., 1969, p. 452.
- V. Venkateswaran: Ph. D. Thesis, The University of British Columbia, 1980.
- K. Huebner: *The Finite Element Method for Engineers*, John Wiley and Sons, New York, NY, 1975, pp. 4, 5.
- V. Voller, M. Cross, and P. Walton: *Numerical Methods in Thermal Problems*, R. Lewis et al., eds., Pineridge Press, Swansea, U. K., 1979, vol. 1, pp. 172-81.
- D. Lynch and K. O'Neill: *Int. J. Numer. Methods Eng.*, 1981, vol. 17, pp. 81-96.
- W. Rolph and K. Bathe: *Int. J. Numer. Methods Eng.*, 1982, vol. 18, pp. 119-34.
- G. Guymon and J. Luthin: *Water Resources Research*, 1974, vol. 10, p. 995.
- E. Lemmon: *Numerical Methods in Heat Transfer*, R. Lewis et al., eds., John Wiley and Sons Ltd., New York, NY, 1981, pp. 201-13.
- S. Del Giudice, G. Comini, and R. Lewis: *Int. J. Numerical Analytical Methods Geomechanics*, 1978, vol. 2, pp. 223-35.
- G. Comini, et al.: *Int. J. Numer. Methods Eng.*, 1974, vol. 8, pp. 613-24.
- G. Keramidas: *2nd International Conference on Numerical Methods in Thermal Problems*, Venice, Italy, July 7-10, 1981, R. Lewis et al., eds., Pineridge Press Ltd., Swansea, 1981, pp. 67-77.
- W. Köhler and J. Pitt: *Int. J. Numer. Methods Eng.*, 1974, vol. 8, pp. 625-31.
- T. Dupont, G. Fairweather, and J. Johnson: *Siam J. Numerical Analysis*, 1974, vol. 11, pp. 392-410.
- M. Hogge: *Numerical Methods in Heat Transfer*, R. Lewis et al., eds., John Wiley and Sons Ltd., 1981, pp. 75-90.
- W. Wood: *Int. J. Numer. Methods Eng.*, 1978, vol. 12, pp. 1717-26.
- M. Lees: *Maths. Comp.*, 1966, vol. 20, pp. 516-22.
- C. Bonaccina and G. Comini: *Int. J. Heat Mass Transfer*, 1973, vol. 16, pp. 581-98.
- K. Morgan, R. Lewis, and J. Williams: *The Mathematics of Finite Elements and Applications III*, Ed. Whiteman, Academic Press, New York, NY, 1979, pp. 319-25.
- J. Crank and P. Nicolson: *Proc. Camb. Philos. Soc.*, 1947, vol. 43, pp. 50-67.
- W. Wood and R. Lewis: *Int. J. Numer. Methods Eng.*, 1975, vol. 9, pp. 679-89.
- E. Wilson, K. Bathe, and F. Peterson: *Nuclear Engineering and Design*, 1974, vol. 29, pp. 110-24.
- K. Bathe and M. Khoshgoftaar: *Nuclear Engineering and Design*, 1979, vol. 51, pp. 389-401.
- M. Hogge and C. Nyseen: *Finite Elements in Nonlinear Mechanics*, Tapir, Trondheim, Norway, 1977, vol. 2, pp. 767-85.
- G. Beer and J. Meek: *Finite Element Methods in Engineering*, Proceedings of the First International Conference in Australia on Finite Element Methods, A. Kabaila and V. Pulmano, eds., Clarendon Press, Kensington, NSW, Australia, 1974, pp. 729-40.
- M. Hogge: *Int. J. Numer. Methods Eng.*, 1980, vol. 16, pp. 51-64.
- G. Forsythe and C. Moler: *Computer Solution of Linear Algebraic Systems*, Prentice Hall, Englewood Cliffs, NJ, 1967.
- W. Gray and N. Schnurr: *Computer Methods in Applied Mechanics and Engineering*, 1975, vol. 6, pp. 243-45.
- A. Emery, K. Sugihara, and A. Jones: *Numerical Heat Transfer*, 1979, vol. 2, pp. 97-113.
- P. Gresho and R. Lee: *Finite Element Methods for Convection Dominated Flows*, Proceedings of the Winter Annual ASME Meeting, New York, NY, Dec. 2-7, 1979, ASME, 1979, pp. 37-60.
- S. Patankar and B. Baliga: *Numerical Heat Transfer*, 1978, vol. 1, pp. 27-37.
- J. Donea: *Int. J. Numer. Methods Eng.*, 1974, vol. 8, pp. 103-10.
- A. Moore, B. Kaplan, and D. Mitchell: *Int. J. Numer. Methods Eng.*, 1975, vol. 9, pp. 938-43.
- A. Emery and W. Carson: *J. Heat Transfer*, Trans. ASME, 1971, vol. 93, pp. 136-45.
- R. Yalamanchili and S. Chu: *J. Heat Transfer*, Trans. ASME, 1973, vol. 95, pp. 235-320.
- R. Sarjant and M. Slack: *J. Iron St. Inst.*, 1954, vol. 177, pp. 428-44.